Quantitative Biology 2022, 10(3): 226–238
https://doi.org/10.15302/J-QB-021-0285

REVIEW

Applications of image analysis in plant chromosome and chromatin structure study

Nobuko Ohmido[1,*], Astari Dwiranti[2], Seiji Kato[1], Kiichi Fukui[3]

[1] Graduate School of Human Development and Environment, Kobe University, Kobe 657-8501, Japan
[2] Cellular and Molecular Mechanisms in Biological System (CEMBIOS) Research Group, Department of Biology, Faculty of Mathematics and Natural Sciences, Universitas Indonesia, Depok Campus, West Java 16424, Indonesia
[3] Graduate School of Pharmaceutical Sciences, Osaka University, Suita, Osaka 565-0871, Japan
* Correspondence: ohmido@kobe-u.ac.jp

Received February 10, 2021; Revised April 7, 2021; Accepted April 26, 2021

***Background*: The use of image analysis to understand the structure of chromosome and chromatin is critical to the study of genetic evolution and diversification. Furthermore, a detailed chromosome map and the structure of chromatin in the nucleus may contribute to the plant breeding and the study of fundamental biology and genetics in organisms.**

***Results*: In plants with a fully annotated genome project, such as the Leguminosae species, the integration of genetic information, including DNA sequence data, a linkage map, and the cytological quantitative chromosome map could further improve their genetic value. The numerical parameters of chromocenters in 3D can provide useful genetic information for phylogenetic studies of plant diversity and heterochromatic markers whose epigenetic changes may explain the developmental and environmental changes in the plant genome. Extended DNA fibers combined with fluorescence *in situ* hybridization revealed the highest spatial resolution of the obtained genome structure. Moreover, image analysis at the nano-scale level using a helium ion microscope revealed the surface structure of chromatin, which consists of chromatin fibers compacted into plant chromosomes.**

***Conclusions*: The studies described in this review sought to measure and evaluate chromosome and chromatin using the image analysis method, which may reduce measurement time and improve resolution. Further, we discussed the development of an effective image analysis to evaluate the structure of chromosome and chromatin. An effective application study of cell biology and the genetics of plants using image analysis methods is expected to be a major propeller in the development of new applications.**

Keywords: CHIAS; chromosome; chromatin; extended DNA fiber; helium ion microscopy; nucleus; plants

Author summary: This review focuses on the development of imaging analysis for the integration chromosome map using chromosome image analyzing system (CHIAS) and fluorescence *in situ* hybridization (FISH) in important crops, *e.g.*, rice and beans. 3D chromatin structures of chromocenters (CCs) in nuclei and extended DNA fibers (EDFs) for the measurement of DNA repeats and gene sizes are informative for plant genetics. Nano scale imaging using the helium ion microscope (HIM) represents new information about chromatin condensation. We demonstrated how imaging applications subjected to plant chromosomes and chromatin are effective in fundamental biology and genetics in plants.

INTRODUCTION

Human visual cues are estimated to account for 70%–80% of all external stimuli received by humans from their surroundings. As a result, information that can be perceived visually is important in the field of quantitative biology. Although visual information is generally extensive and difficult to understand, scientists

have continually sought different approaches to present such information by converting it to numerical values and measurements such as length, angle and area, and the type of visual information used. Some visual information, such as chromosome structure, is particularly difficult to evaluate without a subjective measure of the available information. Consequently, analyses of visual information have posed a challenge for scientists. Because only biological expert researchers can evaluate results with their naked eye, objective evaluation methods are highly demanded. The computer technology has been rapidly developing since the late 20th century. In fact, computers have become very helpful, sometimes even indispensable, tools for research in the field of image analysis; this is because they can be used to process visual information objectively. In the past, due to the high cost and need for dedicated instruments, only few researchers had access to systems for digital image analysis. As image analysis is now popular and necessary in several biology fields, it is important to understand the implications of this approach.

The development of chromosome karyotyping using image analysis is important for genetic evolution and diversification. In fact, a detailed chromosome map is thought to contribute to the plant breeding, and the study of fundamental biology and genetics of organisms. Chromosome mapping is carried out with a locus that allows the band to appear on a chromosome using differential staining techniques, such as G-band or C-band [1]. Forty-six human chromosome identifications representing clear G-bands treated with trypsin have been established [2,3]. Rely on the varying genome sizes among plants species, although individual banding patterns show on the chromosomes of important crops, *e.g.,* wheat (average genome size, 807 Mb/each chromosome [4]), barley (1026 Mb), and field bean (3324 Mb) which are pretty large and easily observed chromosomes, in the comparison of such as rice (41 Mb), *Lotus japonicas* (78 Mb), red clover (63 Mb) and soybean (55 Mb) do not show the clear band patterns. Those species with a small chromosome (less 100 Mb/chromosome) have been able to identify chromosomes by performing image analysis and FISH detection on the typical condensation pattern of chromosomes.

Fukui *et al.* [5] developed first chromosome image analyzing system (CHIAS) and a chromosome map by analyzing the chromatin condensation pattern. A quantitative barley N-banded chromosome map was also developed using CHIAS to integrate both the genetics and chromosome of barley [6]. CHIAS II is an improved version of the original CHIAS. It includes a mainframe upgraded from professional and special equipment to personal software in a PC [7–9]. CHIAS II was also used to develop quantitative chromosome maps [10]. CHIAS II developed to analyze *Brassica* chromosomes and was subsequently used to identify three diploid *Brassica* chromosomes (*B. rapa, B. nigra*, and *B. oleracea*, with AA, BB, and CC genomes, respectively). All chromosomes of *B. napus* ($2n = 38$, AACC genome) were identified by CHIAS II, and a quantitative chromosome map or idiogram was developed. Nevertheless, the image analysis technology was only available to few researchers owing to the absence of affordable image-processing equipment.

Applications of a wide range of visualization procedures in plant genome studies are now essential for obtaining quantitative data on genomes and their evolution. Chromosomal maps are useful for efficient plant genome analysis. To develop a chromosomal map, an image analysis method that performs objective analysis while avoiding human subjective judgments and ambiguous expression, is extremely effective. Previously, a detailed chromosome map was developed for each small plant chromosome [11,12]. Extracting features from an image is common in an image analysis method for gene and genome mapping. Fluorescence *in situ* hybridization (FISH), which involves the labeling of a fluorescent dye to a gene, was previously developed [13]. By transducing the cooled CCD camera that could detect a very small amount of light, the digitization of the chromosome image progressed rapidly, and the affinity with the image analysis became greater. To carry out an effective study of the plant genome, total genomics combined with chromosome image analysis and the FISH method should be performed. Monocotyledon and dicotyledon model plants, such as rice and *Arabidopsis*, were previously subjected to genome projects [11,12]. Integrating the genetic information of DNA sequence and deriving a linkage map and cytological quantitative chromosome map could further improve the genetic value of these plants.

In this review, we evaluated the effectiveness of digitization using the image analysis technology. Chromosome studies are required to establish and certify the importance of imaging methods in the development of new genetic models. Quantitative analysis of chromosomes and chromatins includes information about the correct positional information of a connected chromatin conformation, such as heterochromatin and euchromatin for genomic elucidation; such analysis could be carried out using the image analysis program developed in previous studies. We also sought to describe the development of an image analysis system for small chromosome FISH mapping and karyotyping, nucleus structure, fiber DNA and nano-level chromatin structure using an advanced helium ion microscope. Finally, we

discussed the development of an effective image analysis application for the chromosome and chromatin structure of plants.

IMAGING THE IDIOGRAM OF SMALL PLANT CHROMOSOMES

Small chromosomes in plants such as Gramineae and Leguminosae do not display clear bands in conventional banding methods, such as N and C banding methods. This is because the tiny and similar-sized chromosomes in the mitotic metaphase impedes the identification of individual chromosomes. The morphological characteristics of the chromosomes are difficult to analyze. Therefore, a characteristic condensation pattern (CP) has been reported in prometaphase chromosomes during mitosis in rice [5]. CP is the differentiation between chromatin condensed and non-condensed regions especially in small plant chromosomes at the prometaphase stage. The CP shows the individual characteristic chromosome feathers on each of the 12 chromosomes in rice instead of C-, N-, or G-banding patterns. Using characteristic CP as a parameter for image analysis enables the identification of chromosomes and the construction of a quantitative chromosome map. Chromosomal maps of *Lotus japonicus* and red clover (*Trifolium pratense* L.) have also been prepared using CHIAS III [12]. These maps were continuously upgraded with the latest version of the software (currently CHIAS IV) [14].

Fabaceae syn. Leguminosae, the third-largest family of flowering plants, is comprised of 700 genera and 20,000 species of flowering plants, including the most common type of flowering plant found globally. Fabaceae encompasses various species, such as peas (*Pisum sativum*, 2n = 2x = 14; genome size per haploid, 5000 Mb), alfalfa (*Medicago sativa*, 2n = 2x = 16; genome size per haploid, 1600 Mb), and soybeans (*Glycine max*, 2n = 2x = 40; genome size per haploid, 1100 Mb), whose genomes have been studied for years [15]. Fabaceae plant types exhibit remarkable variety (ranging from small annual herbs to massive tropical trees) [16]. The subfamily, Papilionidae, in Fabaceae has the most pulse crops, including major grain legumes, oilseed crops, forage crops, ornamental crops, medicinal crops, and agroforestry species.

The quantification of chromosome density by CHIAS, *in situ* localization of repetitive sequences, and high-resolution mapping of genes and/or markers by FISH are expected to facilitate the analysis of gene density, segment duplication, and other chromosome rearrangements, and to yield integrated maps for legumes. In particular, chromosome analyses that are applicable for *Lotus japonicas* L. and red clover would help to fabricate a framework for common legume genomics.

L. japonicus is characterized by a small genome (2n = 2x = 12; genome size per haploid, 472 Mb), relatively short life cycle (2–3 months), and ease of genetic manipulation (*e.g.*, transformation as an autogamous diploid plant) [17,18]. Sato *et al.* [19] constructed a high-density genetic linkage map of *L. japonicus* and mapped numerous transformation-competent artificial chromosome (TAC) genomic markers. These markers are indispensable for Leguminosae studies in various fields, including comparative genomics, gene identification, gene isolation, and marker-assisted breeding. Consequently, several microsatellite and simple sequence repeat (SSR) markers, as well as derived cleaved amplified polymorphic sequences (dCAPS), have been genetically and physically mapped onto the *L. japonicus* genome. Ohmido *et al.* [20] integrated quantitative pachytene chromosome maps using six *L. japonicus* chromosomes based on length, centromeric position, heterochromatin, and euchromatin distribution pattern, as well as the position of major repetitive sequences by using FISH and an imaging method in CHIASIII. In addition, they used high-resolution pachytene chromosomes to determine the precise integration between the genetic and physical distances in the *L. japonicus* genome.

Red clover (*Trifolium pratense* L.) is a forage legume and an allogamous diploid plant (2n = 14; 440 Mb). Kataoka *et al.* [21] examined the seven prometaphase chromosomes of red clover using FISH with several repetitive sequences and bacterial artificial chromosomes (BAC). The investigation using specific BAC clones to determine the chromosome specific regions identified by Sato *et al.* [22]. The position of the hybridization signals and the chromosome condensation patterns were quantified using CHIAS IV. Fourteen BAC clones belonging to the seven linkage groups hybridized to individual chromosomes were identified, thereby establishing the relationship between the linkage groups and the karyotype. Quantitative analysis using FISH mapping and chromosome analysis using CHIAS IV enabled the construction of a quantitative idiogram. This idiogram was comprised of a comprehensive chromosome map of red clover chromosome sequences derived from the same chromosome in each individual and the corresponding chromosome sequence in each individual. Based on the findings, chromosomal collinearity was identified among allogamous red clover varieties. This integration of genetic linkage and quantitative chromosome maps should provide valuable insights into allogamous legume genetics.

IMAGING THE GENOME SIZES AND CHROMATIN CONFORMATION IN INTERPHASE NUCLEI

Genome size plays an important role in the evolution of plants and animals as changes in genome size might accompany, if not facilitate, evolutionary adaptation to environmental conditions. Genome sizes have been analyzed via flow cytometry, a method extensively used to determine plant genome size using fluorescence intensity [23]. Plant DNA flow cytometry is a very popular method with applications ranging from basic and applied research to industry. However, image analysis of interphase nuclei is important to understand characteristics chromatin condensation and the structure of nuclei.

How does the nuclei organization and genome sizes relate in plant cells? Both fluorescent and conventional nuclear staining methods can reveal uneven orientation in a nucleus. Previously, the Rabl orientation was believed to be a basic interphase structure of different plant nuclei [24,25]. However, some plant species with genome sizes less than 1×10^4 Mb (2C value), such as *Arabidopsis thaliana* and *Oryza sativa*, are known to have a non-Rabl orientation [26–29]. Small genome species have chromosomes in their interphase nuclei disposed in diffused chromosome territories, without the Rabl arrangement. However, in 2C value larger than 4×10^4 Mb genomes, the chromosomes run in a string-like manner through the nucleus with a Rabl orientation displayed throughout the cell cycle. Dong and Jiang [27] revealed that Gramineae species with larger 2C values, such as wheat, rye, barley and oats, have a clear Rabl nucleus orientation. They also suggested that a relationship exists between Rabl orientation and genome size in maize with middle 2C value and incomplete formation of the Rabl orientation. Plant species with a 2C value larger than 4×10^4 Mb were found to display Rabl orientation. Furthermore, Fujimoto *et al.* [30] demonstrated that *Lilium* and *Fritillaria* plants with over 7×10^4 Mb (2C values) unexpectedly displayed telomere in both hemispheres; however, *H. vulgare* was found to display a deviation in one hemisphere. The images were deconvoluted to obtain clear 3D images using a deconvolution program. Preservation of the nuclear 3D structure was confirmed with the reconstructed 3D images. As a result, the Rabl orientation was found to not represent a common 3D structure of genomic DNA, even in plants with large 2C values. Several studies have indicated that whether the chromosomes adopt a non-Rabl configuration is not dependent on the genome size in plants (Table 1) [30,31]. Nonetheless, an upper limitation of the ratio of DNA volume to nuclear volume exists in plants. In fact, the constant ratio between the DNA volume and nuclear volume should not exceed 3%.

IMAGING THE CHROMOCENTERS AND 3D STRUCTURE OF INTERPHASE NUCLEI

Computational image analysis provides precise, objective, and reproducible quantitative data from images. Images of interphase nuclei have been analyzed using various methods. In fact, both the fluorescent and conventional nuclear staining methods can be used to reveal uneven DNA density in a nucleus. The nucleus at the interphase can be characterized by distinct morphological features and the distribution pattern of certain chromosomal regions, such as chromocenters (CCs). The nuclei at the interphase are well known to exhibit different distribution patterns in their heterochromatic CCs, which can be used as an indicator of the cytological characteristics of each strain, species, or genus in

Table 1 The CHIAS-Straight menu can be found in the menu bar

Macro command	Protocols for measurements
1. Open	Select “File” followed by “Open”; select the fiber-FISH image (Fig. 1B)
2. Set scale	Select “Analyze” followed by “Set Scale”; Enter the distance in pixels based on the magnification of the CCD camera and microscope
3. Select segmented line tool	Set the width of the region of interest in pixels and draw each segment line along the fiber image
4. Straighten	Turn the selected region to the straightened image (Fig. 1C)
5. Select line tool	Measure the intensity of the fluorescent signals and draw a line to measure the selected region
6. Measure	Measure the length and density of the selected line in the straightened image
7. Plot profile	Plot the intensity of the selected line (Fig. 1D)
Save as	Save image data and/or tables as an Excel file

“Fiber_.jar” must be copied into the “plugins” folder found in the “ImageJ” folder. The plug-in files for CHIAS-Straight can be retrieved from the CHIAS website. There is no cost associated with the plugin; however, registration is required before downloading, according to the user instruction. The plugin file ‘CHIAS_st.jar’ must be installed and copied into the ‘plug-ins’ folder found in the ‘ImageJ’ folder. Thereafter, ‘CHIAS-Straight’ is selected on the menu bar to display the command menu (Fig. 1A).

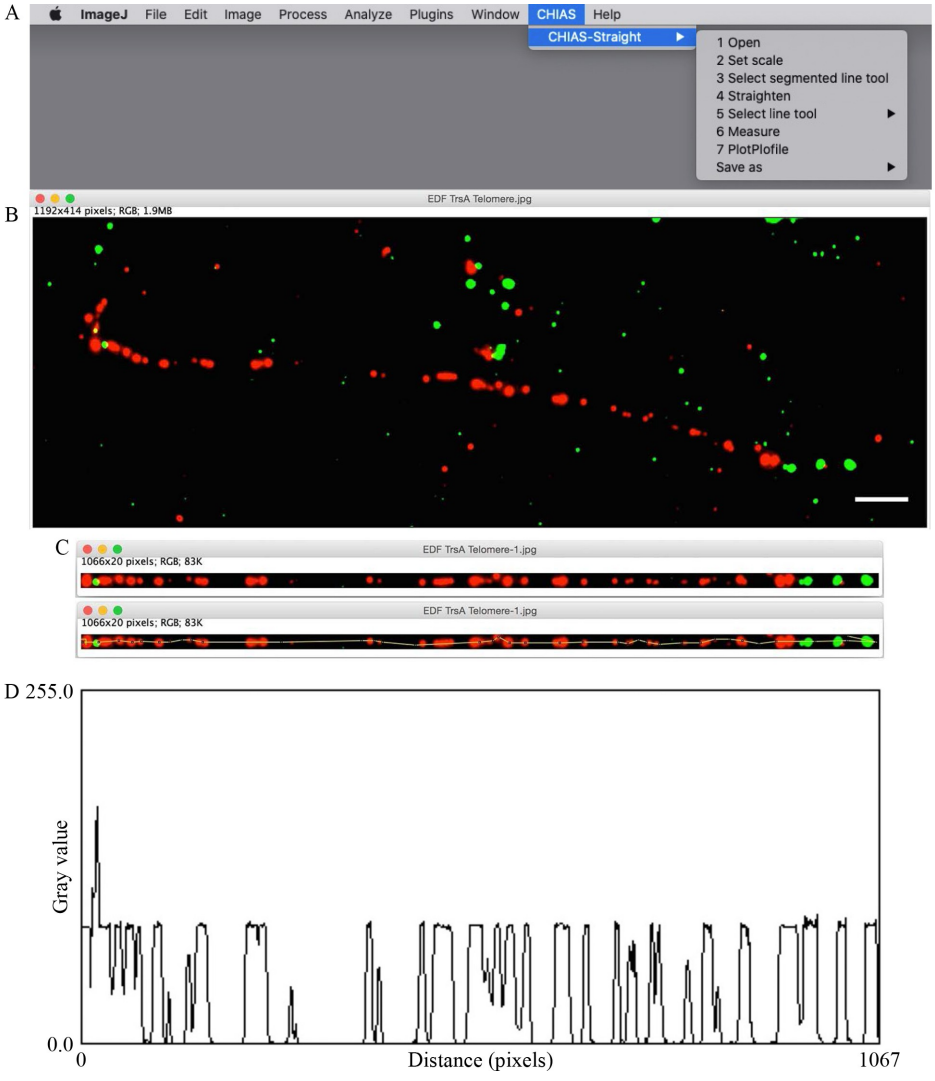

Figure 1. CHIAS-Straight workflow. (A) The menu bar displays the command menu for CHIAS-Straight. (B) Fiber-FISH image with two fluorescent signal colors, red; TrsA, green; telomere. (C) Image of the straightened fiber. (D) Intensity of the fluorescent signals.

plants [32]. In some plants, heterochromatic CCs are displayed as heavily-stained granular regions. Tanaka [33] categorized the distribution patterns of CCs within an interphase nucleus into seven types of "resting chromosomes" in Orchidaceae. As a result, species with a similar form of resting chromosomes would occupy close phylogenic relatives. The numerical parameters of CCs within a nucleus are used to determine the type of resting chromosome, which is a useful cytological characteristic that can serve as an indicator of cross compatibility among plant species. However, it is difficult to objectively determine the size of the types of resting chromosomes through visual inspection of the nuclei under a microscope. Further, individual human biases in the visual determination of the nucleus types cannot be prevented. Quantitative estimation and comparison of the types are almost impossible under normal visual inspection as the comparison of data from different studies cannot be ignored. Acquiring reproducible and quantitative data on the chromocenters within the nucleus is however the most difficult part of objective typing. The image data for the types of resting chromosomes can be separated into four parameters: the number of CCs; area of CCs; percentage of total area of CCs in a nucleus; and distribution of CCs, which are represented by X and Y coordinates for the center of gravity of each CC. The interphase nuclei of Orchidaceae show many CCs with different sizes using conventional aceto-orcein staining methods [25]. An adaptive thresholding method, which was modified with

unsharp mask filtering, was applied previously in the reports [34,35]. Further, this method could be used to analyze the distribution pattern of CCs in the interphase nuclei. The numerical parameters of CCs can provide useful genetic information for phylogenetic studies of plant diversity.

Kikuchi *et al.* [36] observed parental centromere behavior during mitosis and the meiotic prophase. To understand the positioning of parental centromeres in a fertilized egg, genome separation in the nuclei of epidermal cells and apical meristem cells from F_1 hybrids was statistically analyzed between *Torenia fournieri* and *T. baillonii*. To determine the separation between two species centromere signal sets in the nuclei, a 3D distinction computer program [25] was used. FISH with centromere repeats would reveal the relationship between the specific sequence and nuclear structure. Therefore, the separation and association between two parental centromeres in the nuclei of the hybrids were revealed. The 3D program measures and calculates the average nearest distance from a centromere of one species to that of another species in the observed nuclei and digitally-simulated nuclei. The association of centromeres from a single genome was observed at a higher frequency than that with another genome. Such finding suggests that centromeres within one genome are spatially separated from those within the other.

To link nuclear structure and function, imaging tools that quantify nuclear morphology as well as the positioning and organization of chromatin domains in 3D are warranted. Poulet *et al.* [37] performed 3D interphase image analysis using NucleusJ plugin. NucleusJ is an ImageJ plugin in Java language released as a jar file for the ImageJ platform. They examined the shape and size of the nuclei as well as intra-nuclear objects and their position within the nucleus using 3D quantitative measurements from single images or large data sets. Expertise in image analysis with *Arabidopsis* was not required. NucleusJ is useful to users interested in quantifying the size and shape of nuclei, nuclear objects or chromatin domains as well as the positioning of the latter in the nuclear space. The developers expect to improve NucleusJ to quantify FISH and immunochemistry signals and to define automatic segmentation of CCs. NucleusJ can also be adapted to segment FISH signals [37]. Dubos *et al.* [38] introduce the optimized NucleusJ 2.0 to improve the nuclei analyzing speed automated steps. NucleusJ 2.0 was then used to characterize nuclei stained with DNA dyes or labeled with 3D-DNA FISH in whole-mount tissue of a plant mutant with strong alteration of nuclear morphology and chromatin organization.

IMAGING ENVIRONMENTAL EPIGENETICS OF THE INTERPHASE NUCLEI

The CCs in the model plant, *A. thaliana*, are discrete nuclear domains of mainly pericentric heterochromatic regions. Heterochromatin is confined to small pericentromeric regions of all five chromosomes and the nucleolus organizing regions. This clear differentiation enables the study of spatial arrangement and functional properties of individual chromatin domains in the interphase nuclei [39]. Heterochromatin segments are organized as condensed CCs containing heavily cytosine methylated, mainly repetitive DNA sequences. Further, *Arabidopsis* CCs harbor major tandem and dispersed repetitive sequences [39]. Epigenetic markers, such as DNA methylation and histone methylation and acetylation, play vital roles in plant cell growth and development. Differentiated cells exhibit relatively complex histone modification patterns while stem cells display fewer and simpler modifications [40]. Fluorescent protein is also used to visualize specific nuclear protein [41,42]. *Arabidopsis* CCs carry epigenetic markers of silent chromatin, such as histone H3 dimethylated at lysine K9 (H3K9me2) and 5 methyl cytosine (5mC) [39,43]. Immunostaining can also be used to visualize specific molecules modification, such as methylated cytosine and specific nuclear protein development process [44–46], photo response [47], and abiotic stress response [48]. Chromatin plasticity has been proposed to be associated with plant acclimation to environmental changes.

The plant root apical meristem can be divided into three main parts: the meristem, elongation, and maturation zones. There is new evidence that specific epigenetic changes are related to the growth and development of plants. Histone H4 acetylation (H4K5ac), histone H3 methylation (H3K4me2 and H3K9me2), and 5mC have unique and specific patterns in barley meristem tissues [45]. The heterochromatin marker, H3K9me2, has a high concentration in the differentiated cell, boundary meristem-elongation zone, and epidermis cell; however, 5mC is dominant in the root cap and distal meristem. Neither heterochromatin marker is abundant in the proximal meristem region. However, most euchromatin markers (H3K5ac and H3K4me2) are highly concentrated in peri-meristematic regions undergoing highly active cell division. Polosoro *et al.* [48] measured the signal intensities of each histone epigenetic marker on the nuclei of abiotic stress response iron-treated rice plants using CHIAS. Their intensities in proximal meristem nuclei were also compared to those in the elongation zone. Under iron treatment, the concentration

of H3K9me2 increased by approximately 7-fold until its level in the elongation-zone nuclei was identical between control and treated plants. However, the intensity of H3K4me2 in these nuclei declined by approximately 7-fold to levels similar between the two groups of plants. According to a nuclear size analysis by image analysis, the nuclei in the proximal meristem region became smaller and were identical to those in the elongation zone. Regardless of their iron sensitivity, the rice cultivars had generally similar response patterns, which implied that their primary epigenetic responses were similar, although not identical, to those of the other cultivars.

IMAGING THE STRETCHING OF DNA FIBERS

Chromosomes and nuclei consist of DNA fiber, histone proteins, and non-histone proteins [49–51]. The basic unit of chromatin fibers is the nucleosome, which consists of approximately 147 bp of DNA units coiled around a core of octamer histone molecules (two subunits of H2A, H2B, H3, and H4) [52] associated with the linker histone, H1. Nucleosome units connect with other units to form 10-nm fibers, known as "beads on a string" [53]. FISH resolution on the highly condensed somatic metaphase and pachytene chromosomes in plants is estimated to be 4–5 Mb and 1.2 Mb, respectively [54]. Therefore, two DNA sequences located less than 1 Mb apart cannot be reliably resolved. FISH resolution is estimated to be 20–30 kb in human interphase nuclei. Thus, two target sequences that are closer in distance will show overlapped FISH signals on chromosomes and nuclei. To increase the optical restriction of the resolution of light microscopy (about less than 100 nm), *e.g.*, structured illumination microscopy (SIM), photoactivated localization microscopy (PALM), stochastic optical reconstruction microscopy (STORM), and stimulated emission depletion microscopy (STED) offering new insights into molecular structures, interactions and functions of DNA and protein were developed [55]. Recently, Kubalová *et al.* [56] had achieved up to ~4.2-times physically expanded nuclei corresponding to a maximal resolution of ~50–60 nm when imaged by wild-field (WF) microscopy. By applying SIM doubling the WF resolution, the chromatin structures were observed at a resolution of ~25–35 nm.

In contrast to somatic metaphase chromosomes that provide an average resolution of 1 Mb, extended chromatin fibers can be extracted from somatic cells. Fiber-FISH can be used to achieve the highest resolution of mapping of adjacent DNA sequences at distances of only 1 kb [57]. Further, it can be used to achieve a resolution that bridges the megabase molecular techniques, such as pulsed-field gel electrophoresis and sequence analysis of genomes [54]. Fiber-FISH was thus successfully used to perform a detailed investigation of chromosomal domains in *Arabidopsis* [57], rice [58], tomato [59], and sugar beet [60]. By considering the stretching degree of chromatin fibers of 3.27 kb μm^{-1}, multicolor fiber-FISH could be used to measure the physical distance between the DNA sequences in repetitive regions of plant chromosomes, which cannot be assembled in genome sequencing projects. Multicolor FISH on extended DNA fibers (EDFs) allows the placement and visualization of markers, genes, and repetitive sequences on each of the chromosomes that cannot be mapped by recombination-based methods or direct contig assembly.

Stretched chromatin fibers have been used as an effective alternative procedure for mapping adjacent DNA probes with a higher spatial resolution [57,61]. Fiber-FISH was mainly used to analyze the structure and organization of repetitive DNA sequences and determine the length of long DNA molecules [62]. EDFs combined with FISH has the highest spatial resolution for obtaining genome structure; this is because all proteins that interact with DNA compaction are removed and the genome DNAs are extended. This method was used to detect the molecular organization of genome structures. FISH was thus applied to detect in japonica and indica rice [26]. As a result, a rice A genome-specific tandem repeat sequence (TrsA) FISH signals were found to be localized in the terminal regions of the long arms of rice chromosomes. In dual-color FISH experiments on chromosomes, these signals were found to overlap with the telomeric-specific signals in the terminal regions (Fig. 1B). Fiber-FISH enables accurate analysis of repetitive sequences in the eukaryotic genomes and is valuable in large genome sequencing projects. Information for DNA or protein in EDFs and nuclei that can be observed visually, can also be analyzed quantitatively using image analysis methods.

As mentioned above, information for DNA or protein in EDFs and nuclei that can be observed visually, can also be quantitatively analyzed using image analysis methods. CHIAS-Straight can be used to carry out quantitative analysis of fiber signals on EDFs (Fig. 1A). CHIAS-Straight is a free application that is used to measure the imaging performance of fiber-FISH and immunostained chromatin fibers (Fig. 1B, Table 1) [58,60,63]. Routinely, 25–100 signal tracks are screened to measure the length of the fluorescent signal tracks on EDFs (Fig. 1C, D). The CHIAS-Straight plugin file can be installed after a user is registered in the website of Ohmido lab and the CHIAS-Straight manual can be founded in Ohmido lab. CHIAS IV runs as a plug-in in

the public-domain image-processing software, ImageJ (National Institute of Health (NIH) Bethesda, MD, USA) using the Java programming language [64]. ImageJ is the host application for CHIAS IV [14]; for both operating systems, the software requires ImageJ version 1.51 or later.

Fiber-FISH can be employed to carry out an analysis of tandem duplications associated with large genomic duplicates. In fact, fiber-FISH characterization of a 620-kb mitochondrial DNA (mtDNA) fragment inserted into chromosome 2 of *A. thaliana* [65] was achieved early after its introduction. This large mtDNA insert was derived from complex duplication and deletion events, which could not be characterized using traditional methods, such as PCR or southern blot hybridization. Koo *et al.* [66] developed fiber-FISH imaging to detect mtDNA fragments in the nuclear genome. Somatic human cells contain thousands of copies of mtDNA. In eukaryotes, natural transfer of mtDNA into the nucleus generates nuclear mtDNA copies. As a result, Koo and colleagues developed fiber-FISH imaging to carry out mtDNA repeat calculations to analyze nuclear mtDNA insertions in the entire human genome. This method is called mtDNA FIBER-FISH and is employed for cancer cell lines and primary tumors and in advance basic and translational cancer research.

IMAGING THE NANOSTRUCTURE OF PLANT CHROMOSOMES

Chromosome compaction of chromatin fibers results in the formation of a nucleosome consisting of a DNA unit coiled around a core of histone molecules associated with a linker histone. Since the discovery of chromosomes in the 19th century, the compaction of chromatin fibers has been controversial. Moreover, higher levels of chromatin fibers appear as shallow supercoiled 30 nm structures, known as solenoids [67]. Helium ion microscopy (HIM) or scanning helium ion microscope is a state-of-the-art nanofabrication imaging technique that harnesses the positive charge of helium ions interacting on the surface of samples [68]. Owing to the use of high beam energy, this technique allows helium ions to be deposited deep into biological samples as the mass of the ion is greater than that of the electron. As a result, a small beam spot and high secondary electrons (SEs) are produced, thereby demonstrating the brightness of SE emissions [68]. Recently, HIM was used to study the effects of magnesium ions on the structure of the human chromosome, which is composed of 11-nm chromatin fibers. This technology did not require a metal coating owing to sufficient SEs and low beam damage [69]. HIM is thus a powerful tool for nano-level imaging as well as the analysis of the surfaces of biological soft samples. However, HIM has yet to be used to study the structure of plant chromosomes.

Sartsanga *et al.* [70] developed a simple technique to isolate intact barley (*H. vulgare*) chromosomes in high yield. As a result, chromosomes could be observed with a high-resolution scanning ion microscope and the HIM imaging technology, which is based on a scanning helium ion beam. HIM images captured from the surface chromatin fibers of the barley chromosome were analyzed to determine the size and alignment of the chromatin fibers via image analysis. Image analysis was also used to analyze the chromatin fiber images and based on Wako *et al.* [71], chromosome images obtained by HIM were subjected to several imaging processes. A series of steps were carried out to analyze the images obtained by HIM (Fig. 2). Briefly, the area of the chromatin fiber was defined using the HIM image (steps 1 to 3) (Fig. 2A–C). Mid lib lines were then drawn on the chromatin area (steps 4 and 5) (Fig. 2D). In steps 6 to 8, the width lines of the chromatin fiber were drawn perpendicular to the mid lib lines (Fig. 2E). Finally, the size of the width lines from the chromatin area was measured (step 9). The width lines were denoted by various colors based on their lengths (Fig. 2F). The unit size of the chromatin fibers was 11.6 ± 3.5 nm and was closely aligned to the chromatin network model. Such findings suggest that the surface structure of the chromosome consists of a chromatic fiber network [74]. Compacting the surface structure of barley via a chromatin network and observation via HIM are thus powerful tools for investigating chromatin structure. The procedures discussed herein can be applied to other biomaterials, such as the inner structure of the chromatin axis with DNA and protein interactions. Accordingly, we will investigate the outer and inner structures of chromatin in a future study to fully elucidate the process of chromatin compaction in plant chromosome.

The integrity of condensed chromatin is reported to depend on the binding of cations [75]. Calcium and magnesium are the most abundant cations within a cell. In addition, these cations are known to critically contribute to the chromosome condensation process in eukaryotic cells [76]. Previous studies have revealed the decondensed structure of the chromosome following cation depletion [69,77,78]. However, a qualitative data regarding the effects of both ions on chromosome structure are currently available. Previously, Dwiranti *et al.* [77] investigated the effects of Ca^{2+} and Mg^{2+} on the morphology of chromosomes. In addition, the structural changes that occur in chromosome and chromatin after divalent cation depletion were further analyzed quantitatively using the chelating agent, ethylenediaminetetraacetic acid (EDTA). For this purpose, CHIAS was employed to quantitatively

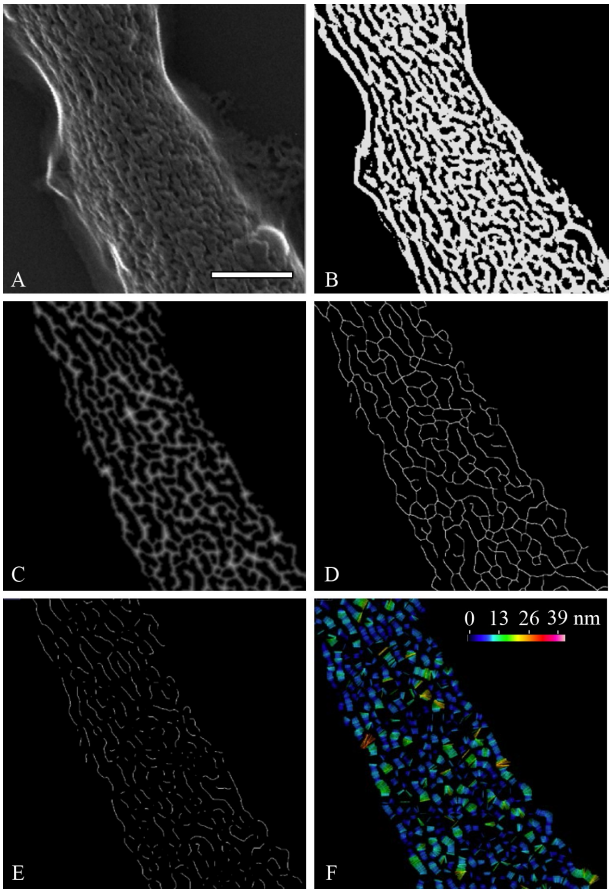

Figure 2. Image analysis based on the procedure used to measure the diameter of chromatin fibers for HIM images [70]. (A) The barley chromosome image was normalized by establishing a range for the gray values: from minimum 0 to maximum 255. (B) The area of the chromatin fiber was defined by the auto local threshold function. (C) The distance map was plotted using white regions in the chamfer distance map found in the MorphoLibJ plugin [72]. Gray values for the area of the chromatin fiber indicate the distance to the black background area. (D) The mid lib lines were calculated from the chromatin area displaying white lines in the Ridge Detection plugin [73]. (E) The junction points were removed from the mid lib lines. (F) The width lines are displayed in different colors based on their lengths. Scale bar = 200 nm. Reprinted with permission.

determine the effect of Ca^{2+} and Mg^{2+} depletion after bent chromosomes were straightened as a result of cation depletion. Successful straightening of the bent chromosomes was achieved using CHIAS IV. Such straightening could also provide quantitative data regarding the chromosome. The average length of the chromosomes was decondensed and double that of the chromosomes treated with EDTA. Collectively, by employing CHIAS IV to straighten the bent chromosomes, the study has demonstrated the effects of cation depletion. Such finding indicates the advantages of CHIAS IV in carrying out chromosome analysis and highlights the fundamental effects of cations on chromosome condensation.

APPLICATION OF OPTICAL IMAGING ANALYSIS FOR NEW PLANT GENOME RESEARCHES

Recent achievements and future applications of genome mapping and oligo-FISH using imaging technology are discussed below. Next-generation genome mapping through fiber-FISH imaging analysis using optical mapping of plant genomes brings genome assemblies to the 'nearly-finished' level for reliable and detailed gene annotations and assessment of structural variations (Gaiero *et al.* 2018). An improved high-throughput optical mapping technology is being applied to image analysis in whole genome mapping [79]. Optical mapping can also be applied to dynamic chromosome structure variations (SVs), such as inversions, deletions, translocations, and duplications. The optical mapping also applied to the genome assembly investigated by the next generation sequence of the large scale scaffold included accurate length information for the direction of the contig and the gap region by combining genome map data, and then misassembled data was corrected. Optical mapping for plant genome analyses has been performed to identify BAC contigs and correct genome assembly errors over the past decade. Optical mapping techniques had been applied in rice [80], medicago [81], maize [82] and tomato [83]. Concerning the identification of the large SVs at chromosomal scale, modern systems based on optical mapping technology such as the Bionano Genomics Saphyr system have remarkable sensitivity towards detection of genome-wide SVs. Shearer *et al.* [83] demonstrated that tomato genome scaffold arrangement based on BAC-FISH and optical mapping changes the positions of hundreds of markers in the linkage map, especially in heterochromatin. These results suggest that similar errors exist in pseudomolecules from other large genomes that have been assembled using only linkage maps to predict scaffold arrangement, and these errors can be corrected using FISH and/or optical mapping. The results of BAC-FISH and optical mapping strongly indicate that many scaffolds were arranged incorrectly, the FISH based arrangement of scaffolds is being used in the new release of the tomato genome. In a role reversal, the new scaffold arrangement based on physical methods should be used to rearrange hundreds of markers in the linkage map. As a result, it is possible to generate and handle the massive quantities of optical mapping data that are

required for the assembly of a large and complex plant genome.

Idziak *et al.* (2014) studied the karyotype evolution of small genome grasses using BAC-FISH based comparative chromosome barcoding in four *Brachypodium* species. The well-developed cytogenetic platform for *Brachypodium* species permits two complementary approaches to comparative mapping—chromosome barcoding and chromosome painting. BAC-FISH-based chromosome barcoding in seven *Solanum* species of the Solanaceae revealed inversions that affect specific lineages of the genus and thus enabled the construction of the ancestral chromosome [84].

An important recent development is the application of FISH probes based on synthetic oligos, which can be used to create synthetic oligos. Oligo based probes can be designed either from repetitive DNA elements or from single-copy DNA sequences, a paradigm shift from the traditional FISH probes using cloned DNA sequences. Oligo probes designed from simple-sequence repeats or satellite repeats synthetic oligo-FISH probes were first developed to physically map simple-sequence repeats (SSRs) in plants [85]. Synthesized oligos specific to specific chromosomal regions, or to an entire chromosome can be computationally identified, synthesized in parallel, and fluorescently labeled. Oligo probes designed from conserved DNA sequences from one species can be used among genetically related species, allowing comparative cytogenetic mapping. The advances in synthetic oligo probes will significantly expand the applications of FISH in many plant and crop species.

CONCLUSIONS

In order to understand the functions of genes and the genome, it is essential to understand the structure of chromosomes and nuclei. To help in the clarification of the taxonomy status of plants, imaging analysis for chromosome ideogram is important. Chromatin conformation and 3D structure analysis could be helpful the genome cosmic nuclei.

Recently, RNA-guided endonuclease—*in situ* labelling (RGEN-ISL) was reported as visualizing instead of FISH [86]. RGEN-ISL is a simple method to visualize repetitive DNA sequences using the CRISPR/Cas9 system. It is versatile and simple to use, and has been used to visualize DNA sequences in nuclei or chromosomes without the denature process which destroys the structures of cytological samples. RGEN-ISL is capable of simultaneously detecting DNA loci and immunohistochemical signals, including histone modification, in various types of plant tissues and species [87].

The studies described in this review sought to measure and evaluate chromosome and chromatin using image analysis methods, which may reduce measurement time and improve resolution. Further, we discussed the development of an effective image analysis to evaluate the structure of chromosome and chromatin in chromosome and nucleus. The study of cell biology and the genetics of plants using image analysis methods is expected to be a major propeller in the development of new applications.

ABBREVIATIONS

FISH	Fluorescence *in situ* hybridization
CCs	Chromocenters
CHIAS	Chromosome image analyzing system
HIM	Helium ion microscopy
CP	Condensation pattern
EDFs	Extended DNA fibers
mtDNA	Mitochondrial DNA
SE	Secondary electrons

ACKNOWLEDGEMENTS

This work was supported by "e-ASIA Joint Research Program", "Development of nano-visualization for structural analyses of genetic materials and early infection process for further innovation of functional bio-nanotechnology" from SICORP, and the Mobility Plus Project (No. JPJSBP 120203507) (to NO). This work was also supported by "The 51st Research Grants in the Natural Sciences" from The Mitsubishi Foundation and Nanotechnology Platform of MEXT (No. JPMXP09F20OS0004 (to NO). We thank the Nanotechnology Open Facilities Center in Osaka University for allowing us to conduct our HIM observation. Further, we would like to thank Dr. Kimihiro Norizawa from Osaka University for all his guidance regarding the HIM technique as well as Editage (www.editage.com) for English language editing.

COMPLIANCE WITH ETHICS GUIDELINES

The authors Nobuko Ohmido, Astari Dwiranti, Seiji Kato and Kiichi Fukui declare that they have no conflict of interest or financial conflicts to disclose.

The article is a review article and does not contain any human or animal subjects performed by any of the authors.

REFERENCES

1. Sumner, A. T., Evans, H. J. and Buckland, R. A. (1971) New technique for distinguishing between human chromosomes. Nat. New Biol., 232, 31−32
2. Caspersson, T., Lomakka, G. and Moller, A. (1972) Computerized chromosome identification by aid of the quinacrine mustard fluorescence technique. Hereditas, 67, 103−110
3. Zahed, L., Murer-Orlando, M. and Bobrow, M. (1989) The application of automated metaphase scanning to direct preparations of chorionic villi. Prenat. Diagn., 9, 7−17
4. Pellicer, J. and Leitch, I. J. (2020) The Plant DNA C-values database (release 7. 1): an updated online repository of plant genome size data for comparative studies. New Phytol., 226, 301−305
5. Fukui, K. (1986) Standardization of karyotyping plant chromosomes by a newly developed chromosome image analyzing system (CHIAS). Theor. Appl. Genet., 72, 27−32
6. Kakeda, K., Fukui, K. and Yamagata, H. (1991) Heterochromatic differentiation in barley chromosomes revealed by C- and N-banding techniques. Theor. Appl. Genet., 81, 144−150
7. Kato, S., Hirose, T., Akiyama, Y., O'neill, C. M. and Fukui, K. (1997) Manual on the chromosome image analyzing system III, CHIAS III. Res. Report Hokuriku Natl. Agr. Exp. Stn., 1–76
8. Nakayama, S. and Fukui, K. (1997) Quantitative chromosome mapping of small plant chromosomes by improved imaging on CHIAS II. Genes Genet. Syst., 72, 35−40
9. Iijima, K., Kakeda, K. and Fukui, K. (1991) Identification and characterization of somatic rice chromosomes by imaging methods. Theor. Appl. Genet., 81, 597−605
10. Fukui, K., Nakayama, S., Ohmido, N., Yoshiaki, H. and Yamabe, M. (1998) Quantitative karyotyping of three diploid Brassica species by imaging methods and localization of 45s rDNA loci on the identified chromosomes. Theor. Appl. Genet., 96, 325−330
11. Fukui, K. and Iijima, K. (1991) Somatic chromosome map of rice by imaging methods. Theor. Appl. Genet., 81, 589−596
12. Ito, M., Ohmido, N., Akiyama, Y. and Fukui, K. (2000) Quantitative chromosome map of A*rabidopsis thaliana* L. by imaging methods. Cytologia (Tokyo), 65, 325−331
13. Langer, P. R., Waldrop, A. A. and Ward, D. C. (1981) Enzymatic synthesis of biotin-labeled polynucleotides: novel nucleic acid affinity probes. Proc. Natl. Acad. Sci. USA, 78, 6633−6637
14. Kato, S., Ohmido, N. and Fukui, K. (2009) Image analysis of small plant chromosomes by using an improved system, CHIAS IV. Chromosome Sci., 12, 43−50
15. Choi, H. K., Mun, J. H., Kim, D. J., Zhu, H., Baek, J. M., Mudge, J., Roe, B., Ellis, N., Doyle, J., Kiss, G. B., *et al*. (2004) Estimating genome conservation between crop and model legume species. Proc. Natl. Acad. Sci. USA., 101, 15289−15294
16. Doyle, J. J. and Luckow, M. A. (2003) The rest of the iceberg. Legume diversity and evolution in a phylogenetic context. Plant Physiol., 131, 900−910
17. Jiang, Q. and Gresshoff, P. M. (1997) Classical and molecular genetics of the model legume *Lotus japonicus*. Mol. Plant Microbe Interact., 10, 59−68
18. Udvardi, M. K., Tabata, S., Parniske, M. and Stougaard, J. (2005) *Lotus japonicus*: legume research in the fast lane. Trends Plant Sci., 10, 222−228
19. Sato, S., Nakamura, Y., Kaneko, T., Asamizu, E., Kato, T., Nakao, M., Sasamoto, S., Watanabe, A., Ono, A., Kawashima, K., *et al*. (2008) Genome structure of the legume, *Lotus japonicus*. DNA Res., 15, 227−239
20. Ohmido, N., Ishimaru, A., Kato, S., Sato, S., Tabata, S. and Fukui, K. (2010) Integration of cytogenetic and genetic linkage maps of *Lotus japonicus*, a model plant for legumes. Chromosome Res., 18, 287−299
21. Kataoka, R., Hara, M., Kato, S., Isobe, S., Sato, S., Tabata, S. and Ohmido, N. (2012) Integration of linkage and chromosome maps of red clover (*Trifolium pratense* L.). Cytogenet. Genome Res., 137, 60−69
22. Sato, S., Isobe, S., Asamizu, E., Ohmido, N., Kataoka, R., Nakamura, Y., Kaneko, T., Sakurai, N., Okumura, K., Klimenko, I., *et al*. (2005) Comprehensive structural analysis of the genome of red clover (*Trifolium pratense* L.). DNA Res., 12, 301−364
23. Dolezel, J. and Bartos, J. (2005) Plant DNA flow cytometry and estimation of nuclear genome size. Ann. Bot., 95, 99−110
24. Avivi, L. and Feldman, M. (1980) Arrangement of chromosomes in the interphase nucleus of plants. Hum. Genet., 55, 281−295
25. Wako, T. and Fukui, K. (2003) Quantitative analysis of nuclear chromocenter in *Spiranthes sinensis* (Pers.) Ames. Bioimages, 11, 97−103
26. Ohmido, N. and Fukui, K. (1997) Visual verification of close disposition between a rice A genome-specific DNA sequence (TrsA) and the telomere sequence. Plant Mol. Biol., 35, 963−968
27. Dong, F. and Jiang, J. (1998) Non-Rabl patterns of centromere and telomere distribution in the interphase nuclei of plant cells. Chromosome Res., 6, 551−558
28. Shaw, P. J., Abranches, R., Paula Santos, A., Beven, A. F., Stoger, E., Wegel, E. and González-Melendi, P. (2002) The architecture of interphase chromosomes and nucleolar transcription sites in plants. J. Struct. Biol., 140, 31−38
29. Prieto, P., Shaw, P. and Moore, G. (2004) Homologue recognition during meiosis is associated with a change in chromatin conformation. Nat. Cell Biol., 6, 906−908
30. Fujimoto, S., Ito, M., Matsunaga, S. and Fukui, K. (2005) An upper limit of the ratio of DNA volume to nuclear volume exists in plants. Genes Genet. Syst., 80, 345−350
31. Schubert, I. and Shaw, P. (2011) Organization and dynamics of plant interphase chromosomes. Trends Plant Sci., 16, 273−281
32. Nagl, W. (1979) Ultrastructure; condensed chromatin in plants is species-specific (karyotypical) but not tissue-specific (functional). Protoplasma, 100, 53−71
33. Tanaka, R. (1971) Types of resting nuclei in Orchidaceae. Not.

Mag., 84, 118−122
34. Ishida, M., Frank, P., Doi, K. and Lehr, J. (1983) High quality digital radiographic images: improved detection of low-contrast objects and preliminary clinical studies. Radiographics, 3, 325–328
35. Fukui, K., Tsujimoto, H. and Noda, K. (1988) Imaging techniques for wheat karyotyping. In: Proc. 7th. Intl. Wheat Genet. Symp., pp. 275−280
36. Kikuchi, S., Tanaka, H., Wako, T. and Tsujimoto, H. (2007) Centromere separation and association in the nuclei of an interspecific hybrid between *Torenia fournieri* and *T. baillonii* (Scrophulariaceae) during mitosis and meiosis. Genes Genet. Syst., 82, 369−375
37. Poulet, A., Arganda-Carreras, I., Legland, D., Probst, A. V., Andrey, P. and Tatout, C. (2015) NucleusJ: an ImageJ plugin for quantifying 3D images of interphase nuclei. Bioinformatics, 31, 1144−1146
38. Dubos, T., Poulet, A., Gonthier-Gueret, C., Mougeot, G., Vanrobays, E., Li, Y., Tutois, S., Pery, E., Chausse, F., Probst, A. V., *et al*. (2020) Automated 3D bio-imaging analysis of nuclear organization by NucleusJ 2. 0. Nucleus, 11, 315−329
39. Fransz, P., De Jong, J. H., Lysak, M., Castiglione, M. R. and Schubert, I. (2002) Interphase chromosomes in *Arabidopsis* are organized as well defined chromocenters from which euchromatin loops emanate. Proc. Natl. Acad. Sci. USA, 99, 14584−14589
40. Yan, S., Zhang, Q., Li, Y., Huang, Y., Zhao, L., Tan, J., He, S. and Li, L. (2014) Comparison of chromatin epigenetic modification patterns among root meristem, elongation and maturation zones in maize (*Zea mays* L.). Cytogenet. Genome Res., 143, 179−188
41. Matsunaga, S., Nobuko, O. and Kukui, F. (2006) Tabacco NY-2 cells: from cellular dynamics to omics. In: Biotechnology in Agriculture and Forestry, Nagata, T., Matsuoka, K. and Inze, D. (eds.). Springer-Verlag Berlin Heidelberg, Vol. 8, pp. 51–63
42. Kurihara, D., Matsunaga, S., Omura, T., Higashiyama, T. and Fukui, K. (2011) Identification and characterization of plant Haspin kinase as a histone H3 threonine kinase. BMC Plant Biol., 11, 73
43. Soppe, W. J., Jasencakova, Z., Houben, A., Kakutani, T., Meister, A., Huang, M. S., Jacobsen, S. E., Schubert, I. and Fransz, P. F. (2002) DNA methylation controls histone H3 lysine 9 methylation and heterochromatin assembly in *Arabidopsis*. EMBO J., 21, 6549−6559
44. van Zanten, M., Koini, M. A., Geyer, R., Liu, Y., Brambilla, V., Bartels, D., Koornneef, M., Fransz, P. and Soppe, W. J. (2011) Seed maturation in *Arabidopsis thaliana* is characterized by nuclear size reduction and increased chromatin condensation. Proc. Natl. Acad. Sci. USA, 108, 20219−20224
45. Braszewska-Zalewska, A. and Hasterok, R. (2013) Epigenetic modifications of nuclei differ between root meristematic tissues of *Hordeum vulgare*. Plant Signal Behav., 8
46. Braszewska-Zalewska, A. J., Wolny, E. A., Smialek, L. and Hasterok, R. (2013) Tissue-specific epigenetic modifications in root apical meristem cells of *Hordeum vulgare*. PLoS One, 8, e69204
47. Tessadori, F., van Zanten, M., Pavlova, P., Clifton, R., Pontvianne, F., Snoek, L. B., Millenaar, F. F., Schulkes, R. K., van Driel, R., Voesenek, L. A., *et al*. (2009) Phytochrome B and histone deacetylase 6 control light-induced chromatin compaction in *Arabidopsis thaliana*. PLoS Genet., 5, e1000638
48. Polosoro, A., Enggarini, W. and Ohmido, N. (2019) Global epigenetic changes of histone modification under environmental stresses in rice root. Chromosome Res., 27, 287−298
49. Pooley, A. S., Pardon, J. F. and Richards, B. M. (1974) The relation between the unit thread of chromosomes and isolated nucleohistone. J. Mol. Biol., 85, 533−549
50. Skinner, L. G. and Ockey, C. H. (1971) Isolation, fractionation and biochemical analysis of the metaphase chromosomes of *Microtus agrestis*. Chromosoma, 35, 125−142
51. Huberman, J. A. and Attardi, G. (1966) Isolation of metaphase chromosomes from HeLa cells. J. Cell Biol., 31, 95−105
52. Segal, E., Fondufe-Mittendorf, Y., Chen, L., Thåström, A., Field, Y., Moore, I. K., Wang, J. P. and Widom, J. (2006) A genomic code for nucleosome positioning. Nature, 442, 772−778
53. Baldi, S., Korber, P. and Becker, P. B. (2020) Beads on a string-nucleosome array arrangements and folding of the chromatin fiber. Nat. Struct. Mol. Biol., 27, 109−118
54. Hans de Jong, J., Fransz, P. and Zabel, P. (1999) High resolution FISH in plants—techniques and applications. Trends Plant Sci., 4, 258−263
55. Schubert, V. (2017) Super-resolution microscopy—applications in plant cell research. Front Plant Sci, 8, 531
56. Kubalová, I., Schmidt Černohorská, M., Huranová, M., Weisshart, K., Houben, A. and Schubert, V. (2020) Prospects and limitations of expansion microscopy in chromatin ultrastructure determination. Chromosome Res., 28, 355−368
57. Fransz, P. F., Alonso-Blanco, C., Liharska, T. B., Peeters, A. J. M., Zabel, P. and Jong, J. H. (1996) High-resolution physical mapping in *Arabidopsis thaliana* and tomato by fluorescence *in situ* hybridization to extended DNA fibres. Plant J., 9, 421−430
58. Ohmido, N., Kijima, K., Ashikawa, I., de Jong, J. H. and Fukui, K. (2001) Visualization of the terminal structure of rice chromosomes 6 and 12 with multicolor FISH to chromosomes and extended DNA fibers. Plant Mol. Biol., 47, 413−421
59. Szinay, D., Chang, S. B., Khrustaleva, L., Peters, S., Schijlen, E., Bai, Y., Stiekema, W. J., van Ham, R. C., de Jong, H. and Klein Lankhorst, R. M. (2008) High-resolution chromosome mapping of BACs using multi-colour FISH and pooled-BAC FISH as a backbone for sequencing tomato chromosome 6. Plant J., 56, 627−637
60. Dechyeva, D. and Schmidt, T. (2006) Molecular organization of terminal repetitive DNA in Beta species. Chromosome Res., 14, 881−897
61. Jackson, S. A., Wang, M. L., Goodman, H. M. and Jiang, J. (1998) Application of fiber-FISH in physical mapping of *Arabidopsis thaliana*. Genome, 41, 566−572
62. Jiang, J. and Gill, B. S. (2006) Current status and the future of

fluorescence *in situ* hybridization (FISH) in plant genome research. Genome, 49, 1057−1068
63. Ohmido, N., Wako, T., Kato, S. and Fukui, K. (2016) Image analysis of DNA fiber and nucleus in plants. Methods Mol. Biol., 1469, 171−180
64. Abramhoff, M. D., Magelhaes, P. J. and Ram, S. J. (2004) Image processing with ImageJ. Biophoton. Int., 11, 36−42
65. Stupar, R. M., Lilly, J. W., Town, C. D., Cheng, Z., Kaul, S., Buell, C. R. and Jiang, J. (2001) Complex mtDNA constitutes an approximate 620-kb insertion on *Arabidopsis thaliana* chromosome 2: implication of potential sequencing errors caused by large-unit repeats. Proc. Natl. Acad. Sci. USA, 98, 5099−5103
66. Koo, D. H., Singh, B., Jiang, J., Friebe, B., Gill, B. S., Chastain, P. D., Manne, U., Tiwari, H. K. and Singh, K. K. (2018) Single molecule mtDNA fiber FISH for analyzing numtogenesis. Anal. Biochem., 552, 45−49
67. McGhee, J. D., Nickol, J. M., Felsenfeld, G. and Rau, D. C. (1983) Higher order structure of chromatin: orientation of nucleosomes within the 30 nm chromatin solenoid is independent of species and spacer length. Cell, 33, 831−841
68. Joens, M. S., Huynh, C., Kasuboski, J. M., Ferranti, D., Sigal, Y. J., Zeitvogel, F., Obst, M., Burkhardt, C. J., Curran, K. P., Chalasani, S. H., *et al*. (2013) Helium Ion Microscopy (HIM) for the imaging of biological samples at sub-nanometer resolution. Sci. Rep., 3, 3514
69. Dwiranti, A., Hamano, T., Takata, H., Nagano, S., Guo, H., Onishi, K., Wako, T., Uchiyama, S. and Fukui, K. (2014) The effect of magnesium ions on chromosome structure as observed by helium ion microscopy. Microsc. Microanal., 20, 184−188
70. Sartsanga, C., Phengchat, R., Fukui, K., Wako, T. and Ohmido, N. (2021) Surface structures consisting of chromatin fibers in isolated barley (*Hordeum vulgare)* chromosomes revealed by helium ion microscopy. Chromosome Res., 29, 81−94
71. Wako, T., Yoshida, A., Kato, J., Otsuka, Y., Ogawa, S., Kaneyoshi, K., Takata, H. and Fukui, K. (2020) Human metaphase chromosome consists of randomly arranged chromatin fibres with up to 30-nm diameter. Sci. Rep., 10, 8948
72. Legland, D., Arganda-Carreras, I. and Andrey, P. (2016) MorphoLibJ: integrated library and plugins for mathematical morphology with ImageJ. Bioinformatics, 32, 3532−3534
73. Steger, C. (1998) An unbiased detector of curvilinear structures. IEEE PAMI, 20, 113−125
74. Poirier, M. G. and Marko, J. F. (2002) Mitotic chromosomes are chromatin networks without a mechanically contiguous protein scaffold. Proc. Natl. Acad. Sci. USA, 99, 15393−15397
75. Engelhardt, M. (2004) Condensation of chromatin in situ by cation-dependent charge shielding and aggregation. Biochem. Biophys. Res. Commun., 324, 1210−1214
76. Strick, R., Strissel, P. L., Gavrilov, K. and Levi-Setti, R. (2001) Cation-chromatin binding as shown by ion microscopy is essential for the structural integrity of chromosomes. J. Cell Biol., 155, 899−910
77. Dwiranti, A., Takata, H. and Fukui, K. (2019) Reversible changes of chromosome structure upon different concentrations of divalent cations. Microsc. Microanal., 25, 817−821
78. Phengchat, R., Takata, H., Morii, K., Inada, N., Murakoshi, H., Uchiyama, S. and Fukui, K. (2016) Calcium ions function as a booster of chromosome condensation. Sci. Rep., 6, 38281
79. Dong, Y., Xie, M., Jiang, Y., Xiao, N., Du, X., Zhang, W., Tosser-Klopp, G., Wang, J., Yang, S., Liang, J., *et al*. (2013) Sequencing and automated whole-genome optical mapping of the genome of a domestic goat (*Capra hircus*). Nat. Biotechnol., 31, 135−141
80. Zhou, S., Bechner, M. C., Place, M., Churas, C. P., Pape, L., Leong, S. A., Runnheim, R., Forrest, D. K., Goldstein, S., Livny, M., *et al*. (2007) Validation of rice genome sequence by optical mapping. BMC Genomics, 8, 278
81. Young, N. D., Debellé, F., Oldroyd, G. E., Geurts, R., Cannon, S. B., Udvardi, M. K., Benedito, V. A., Mayer, K. F., Gouzy, J., Schoof, H., *et al*. (2011) The Medicago genome provides insight into the evolution of rhizobial symbioses. Nature, 480, 520−524
82. Zhou, S., Wei, F., Nguyen, J., Bechner, M., Potamousis, K., Goldstein, S., Pape, L., Mehan, M. R., Churas, C., Pasternak, S., *et al*. (2009) A single molecule scaffold for the maize genome. PLoS Genet., 5, e1000711
83. Shearer, L. A., Anderson, L. K., de Jong, H., Smit, S., Goicoechea, J. L., Roe, B. A., Hua, A., Giovannoni, J. J. and Stack, S. M. (2014) Fluorescence *in situ* hybridization and optical mapping to correct scaffold arrangement in the tomato genome. G3 (Bethesda), 4, 1395−1405
84. Lou, Q., Iovene, M., Spooner, D. M., Buell, C. R. and Jiang, J. (2010) Evolution of chromosome 6 of *Solanum* species revealed by comparative fluorescence *in situ* hybridization mapping. Chromosoma, 119, 435−442
85. Jiang, J. (2019) Fluorescence *in situ* hybridization in plants: recent developments and future applications. Chromosome Res., 27, 153−165
86. Ishii, T., Schubert, V., Khosravi, S., Dreissig, S., Metje-Sprink, J., Sprink, T., Fuchs, J., Meister, A. and Houben, A. (2019) RNA-guided endonuclease—*in situ* labelling (RGEN-ISL): a fast CRISPR/Cas9-based method to label genomic sequences in various species. New Phytol., 222, 1652−1661
87. Nagaki, K. and Yamaji, N. (2020) Decrosslinking enables visualization of RNA-guided endonuclease—*in situ* labeling signals for DNA sequences in plant tissues. J. Exp. Bot., 71, 1792−1800